Scientific Herald of Uzhhorod University Series “Physics”

Journal homepage: https://physics.uz.ua/en

Issue 51, 39-47

Received: 11.04.2022. Revised: 25.05.2022. Accepted: 15.06.2022

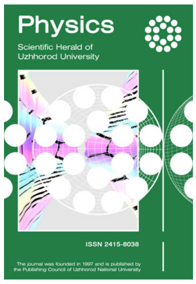

UDC 53.043, 532.5, 533.6.01, 533.16, 533.17
PACS 47.10.-g, 47.32.-y
DOI: 10.54919/2415-8038.2022.51.39-47

Effects of Repulsion and Attraction between Rotating Cylinders in Fluids

Vadym Ostanin*

Abstract

Relevance. From the theory of hydrodynamics, it is known about the interaction of a pair of vortices in inviscid fluids. The relevance of the study is conditioned upon the presence of many studies of numerical simulations of the interactions of two vortices or two cylinders, but the lack of research of practical installations for observing the effects of attraction and repulsion in fluid media may slow down research in this area for practical application.

Purpose. The purpose of this study is a practical demonstration of the possibility of the effect of double interaction in the air, with the calculation of the approximate magnitude of the force tending to attract or repel each of the cylinders.

Methods. In a practical experiment, a pair of plastic cylinders are used, which are driven by engines and rotate next to each other in the air at atmospheric pressure. Numerical simulation of the effect shows the nature of the effect and allows predicting the magnitude of the force generated by rotating cylinders on each other. The relationship between the directions of rotation of the cylinders and the observed effects was verified by numerical simulation using numerical simulation of finite volumes of OpenFOAM version 9.

Results. In a practical experiment, a pair of rotating cylinders started interacting at 5-7 cm in the experiment, which at a smaller distance of 2-3 cm created sufficient force to stabilise the vibrations of one of the cylinders around the thread for which it is suspended. Numerical simulation shows that a zone of high or low pressure is formed in the space between the cylinders, depending on the direction of rotation. The rotation of adjacent disks with opposite directions of rotation helps the circulation of the other cylinder to maintain the flow velocity in the gap, which reduces the fluid pressure between the rotating disks and attracts them. Conversely, rotating disks with the same direction extinguish and compress fluid flows in the gap, which increases the air pressure between rotating objects above the stationary pressure and repels them.

Conclusions. The results of the study provide a better understanding of the processes of fluid interaction, link the dependence of the interaction force on the parameters of the medium and cylinders, and demonstrate the practical possibility of applying the effects of interaction in fluid media

Keywords: interaction of circulations, fluid vortices, cylinder rotation, numerical simulation

Suggested Citation:
Ostanin V. Effects of repulsion and attraction between rotating cylinders in fluids. *Scientific Herald of Uzhhorod University. Series “Physics”*. 2022;(51):39-47.

*Corresponding author

Introduction

Inspired by the similarity of the effects of electromagnetism and rotating vortices [1; 2], and the presence of studies of vortices for water and air environments in the 19-20 centuries [3; 4], the author found most studies using only numerical simulations to describe vortices [5-7]. This paper describes a practical experiment of controlled attraction and repulsion of rotating objects in the air, shows the possibility of practical use of these interactions, and applies numerical simulation to determine the interaction forces using kinetic pressure values. The practical experiment was performed in an air stationary environment at atmospheric pressure. This effect can be a solution for the engineering problem of contactless interaction between objects, when electric or magnetic fields can adversely affect the engineering mission.

Materials and Methods

The equipment for the experiment (Fig. 1) involved two smooth plastic cylinders with a diameter of 50 mm and a length of 100 mm. They were driven by two independent motors from used hard drives, powered by a 12-volt DC source via controllers for brushless motors designed to consume no more than 1.5 amperes. One of the cylinders was suspended on a thin wire to the frame, and the second was in a free position for manipulating it with a hand. The suspended position of one of the cylinders was chosen to capture a weak effect. The wire was used instead of a thread to reduce the unwinding of the cylinder due to the properties of the thread to unwinding under tension. The air around the installation played the role of a viscous medium through which the cylinders interacted. The air was stationary with an atmospheric pressure of 769 mmHg and a temperature of 25°C. The geometric dimensions of the cylinders, the rotation speed, and the air conditions were used to calculate the Reynolds number (1) for practical experiment. When both engines were turned on, the cylinders were unwound to a stable speed of approximately revolutions per minute, which is equal to 26.2 m/s. The rotation speed was measured by a digital tachometer with an accuracy of 0.05%.

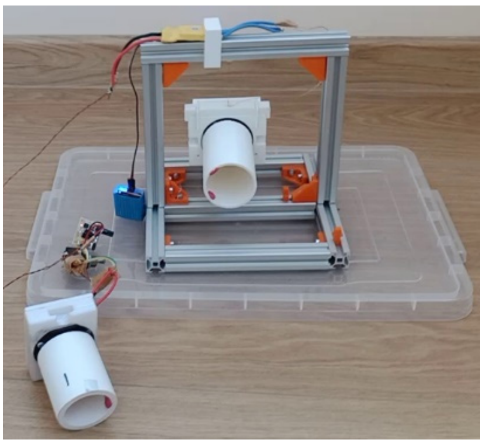

Figure 1. Experimental equipment

$$Re_{air_{\varnothing}} = \frac{\rho_{air}\Omega\mathcal{R}^2}{\eta_{air}} = \frac{1.185 \times 1047 \times 0.025^2}{15.6 \times 10^{-6}} = 49{,}707 \quad (1)$$

where R_{cyl} is the radius of the cylinder = 0.025 m; L_{cyl} is the cylinder length = 0.1 m; Ω is the cylinder rotation speed = = 10^4 *RPM*=167 *RPS*= 1,047 rad/s; ρ_{air} is the air density at 25°C = 1.185 kg/m^3; μ_{air} is the kinematic viscosity [8] of air at 25°C =15.6×10^{-6} m^2/s; η_{air} is the dynamic viscosity of air = = $\rho_{air} \times \mu_{air}$=18.3×10^{-6} kg/(m×s).

Having put each cylinder into rotation (Fig. 2), a boundary layer of air would form on the rotating body of rotation due to the condition of adhesion to the surface of the body with the effect of "no slip condition", which means that at the boundary of a solid object, a viscous liquid flows at zero velocity relative to this boundary (Fig. 3). When each cylinder rotates, this creates a very thin "boundary layer" around the cylinder, the air next to the cylinder simply rotates with it at the same speed (Fig. 4). The cylinder literally drags air with it. And in the next layers, rotation in a viscous medium creates a vortex-free circulation of the flow in a circle around the cylinder.

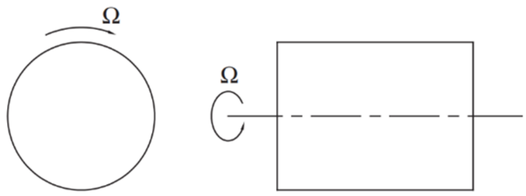

Figure 2. Geometry of the rotating cylinder
Source: [9]

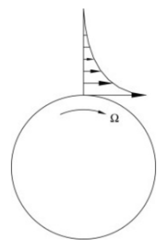

Figure 3. Boundary layer above the rotating disk
Source: [9]

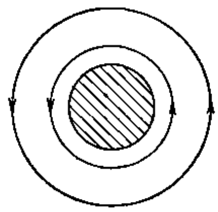

Figure 4. Circulation around the cylinder
Source: [9]

To confirm the causes of the observed effects, OpenFOAM version 9 numerical simulation software with the PISO algorithm was used. The results of calculations and graphs were obtained after a simulation lasting 40 seconds. The results of 4 simulations are presented in this paper. The difference between simulations is presented in Table 1.

Table 1. Boundary layer and environment parameters for different simulations in OpenFOAM9

Name	Boundary layer conditions in simulation of one of two cylinders (file 0.orig/U)	Parameters of kinematic viscosity and medium pressure (transportProperties file)

Attraction in the air	code
	#{
	const fvPatch& boundaryPatch = patch();
	const vectorField& Cf = boundaryPatch.Cf();
	vectorField rot(Cf.size(), vector(0,0,0));
	rot = -10000.0/60*6.28*vector(0,0,1)^(Cf-vector(0.075,0.0, 0.0));
	operator==(rot);
	#};
		transportModel Newtonian;
		nu nu [0 2 -1 0 0 0 0] 1.56e-05;
		rho rho [1 -3 0 0 0 0 0] 1.185;

Repulsion in the air	code
	#{
	const fvPatch& boundaryPatch = patch();
	const vectorField& Cf = boundaryPatch.Cf();
	vectorField rot(Cf.size(), vector(0,0,0));
	rot = 10000.0/60*6.28*vector(0,0,1)^(Cf-vector(0.075,0.0, 0.0));
	operator==(rot);
	#};
		transportModel Newtonian;
		nu nu [0 2 -1 0 0 0 0] 1.56e-05;
		rho rho [1 -3 0 0 0 0 0] 1.185;

Attraction in water	code
	#{
	const fvPatch& boundaryPatch = patch();
	const vectorField& Cf = boundaryPatch.Cf();
	vectorField rot(Cf.size(), vector(0,0,0));
	rot = -10000.0/60*6.28*vector(0,0,1)^(Cf-vector(0.075,0.0, 0.0));
	operator==(rot);
	#};
		transportModel Newtonian;
		nu nu [0 2 -1 0 0 0 0] 0.903e-06;
		rho rho [1 -3 0 0 0 0 0] 997.3;

Repulsion in water	code
	#{
	const fvPatch& boundaryPatch = patch();
	const vectorField& Cf = boundaryPatch.Cf();
	vectorField rot(Cf.size(), vector(0,0,0));
	rot = 10000.0/60*6.28*vector(0,0,1)^(Cf-vector(0.075,0.0, 0.0));
	operator==(rot);
	#};
		transportModel Newtonian;
		nu nu [0 2 -1 0 0 0 0] 0.903e-06;
		rho rho [1 -3 0 0 0 0 0] 997.3;

Results and Discussion

At the first start, the cylinder motors rotated in one direction, the manual cylinder was brought to the hanging cylinder and at about 7 cm or less, the hanging cylinder was repelled from the manual cylinder. The closer the hand cylinder approached, the more the hanging cylinder was repelled, and the force generated by the flows was sufficient to keep the hanging cylinder from meeting the hand cylinder, and not allow the hanging one to return to the equilibrium position of the stretched wire (Fig. 5).

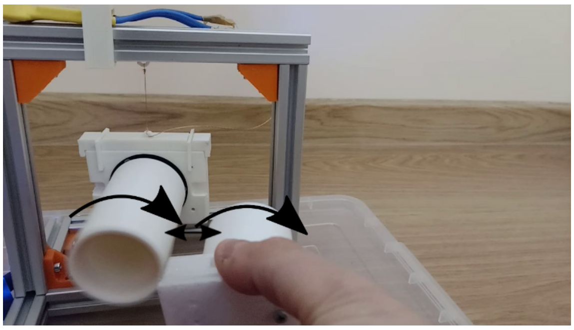

Figure 5. Demonstration of repulsion

Source: [9]

Changing the experimental conditions and rotating the cylinders in opposite directions, the manual cylinder was also brought to the hanging cylinder. Therewith, the attraction of the hanging cylinder to the manual cylinder was observed at a distance of 5 cm or less (Fig. 6). Not removing the manual cylinder in time often led to contact and unbalancing of the hanging cylinder.

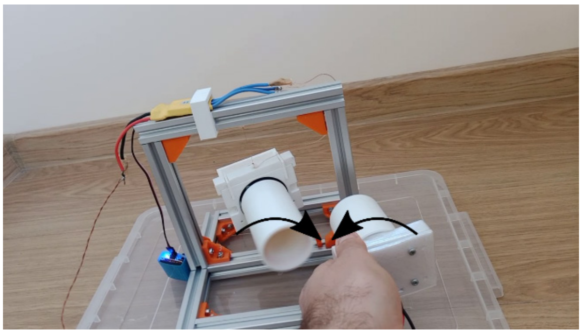

Figure 6. Demonstration of attraction

When the hanging cylinder was unbalanced, to perform several experiments in a row, it was necessary either to stop the hanging cylinder to balance it and start it slowly, or to slow down its rotation on the thread by repulsion or attraction in the air. This was achieved faster with mutual repulsion than with mutual attraction. The force of mutual attraction increased with the approaching, and without prompt removal of the manual cylinder, their collision led to an imbalance of the hanging cylinder. The high speed of rotation and the lack of support points did not allow reducing the distance between the cylinders less than 3 mm.

The vortices created by the cylinders are similar to vortices generated under the water column in streams with a negative longitudinal velocity gradient near the solid boundary [10]. A pair of natural vortices were unstable [11] and tended to unite with unidirectional rotation [12], and with the opposite rotation, destruction caused the development of the Crow instability, which leads to multiple curvatures of the vortices [13]. Similar processes and results were demonstrated by E. Dormy and H.K. Moffatt [14]. They describe the behaviour of medium flows in conditions of short distance, contact, and negative distance between two cylinders. At the point of contact, the total interaction force F, comprising viscosity forces, pressure forces and contact forces, is F_c zero.

Simulation of a single cylinder

As the velocity of the boundary layers increased, the viscous airflow flowed around the cylinder, forming separate vortex-free airflow circulations in the form of concentric circles [15; 16] (Fig. 7). With a sharp start of rotation of the cylinder, vortex flows may be observed at first, but after a few seconds the circulation became vortex-free. Viscous friction considerably affects the behaviour of the medium. Due to the forces of viscous friction, the circulation of fluid flows occurred around a rotating cylinder. In the boundary zone of the air and the cylinder, the pressure was the lowest due to the high flow velocity (2), which is consistent with the Bernoulli equation for viscous fluids:

$$P_1 + \rho g h_1 + \frac{\rho {v_1}^2}{2} = P_2 + \rho g h_2 + \frac{\rho v_2^2}{2} + h_L \qquad (2)$$

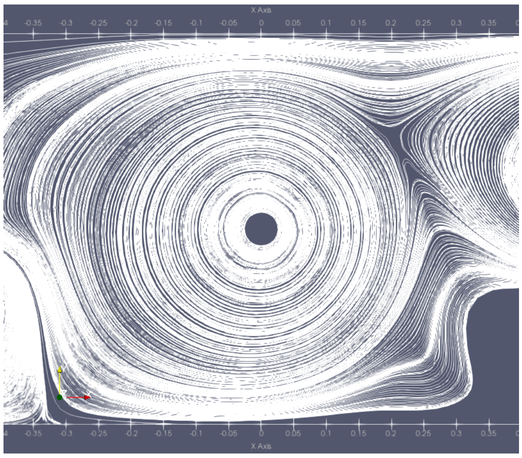

Figure 7. Circulation of one cylinder in a simulation with a rotation speed of 10^4 rpm

The velocity of fluid circulation around the cylinder is inversely proportional to the distance from the cylinder r^2 (3) (Fig. 8).

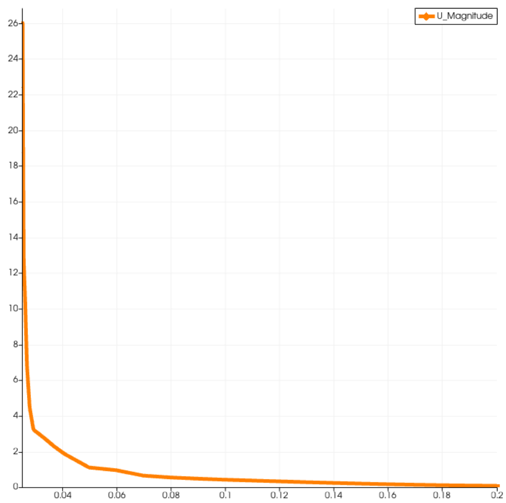

Figure 8. Distribution of the circulation velocity around one cylinder in the simulation at a speed of 10^4 rpm

$$U \sim \frac{1}{r^2} \qquad (3)$$

When rotating, the cylinder carries away the adjacent layers of air, causing its circulation. Vortex-free circulations of a viscous medium cover the entire space outside the cylinder, provided that the space around is boundless. But if the space is limited, e.g., by walls, then swirls occur near the walls. But the flow velocity in these vortices was much less than the main flow near the cylinder, so they were not considered in the observations of effects. The greater the viscous friction, the more stable the circulation, and the slower the circulation rate decreases, moving away from the cylinder. The velocity of the fluid flow was different at the walls and away from them. If one enters the transverse (perpendicular to the velocity vector) coordinate of the distance from the cylinder surface *r*, then the fluid velocity is a function of this distance v(*r*) (Fig. 6). This dependence is determined by the transmission of momentum in the transverse direction or otherwise by the velocity gradient, as in the case of a viscous gas (4):

$$J_p = -\eta \times \frac{dv}{dr} \quad (4)$$

The interaction force of adjacent layers touching on the surface S is equal to (5):

$$F = \eta \times \frac{dv}{dx} \times S \quad (5)$$

Moving away from the cylinders, the circulation rate decreases, keeping the pressure close to stationary, which is higher relative to the cylinder (Fig. 9).

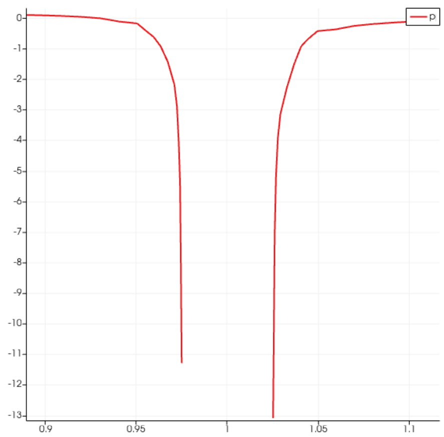

Figure 9. Distribution of kinematic pressure of one cylinder in the simulation

Preparation of the grid for simulation

In the area near the cylinder surface where higher accuracy is required, a fine mesh is used. Moving away from the surface, the mesh becomes rougher (Fig. 10).

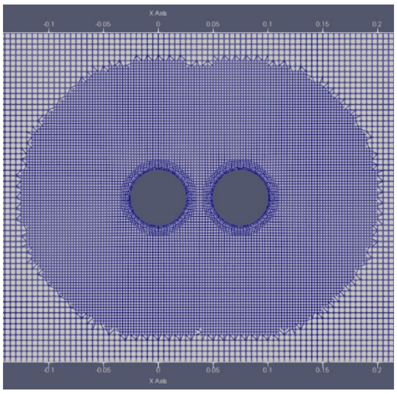

Figure 10. Computational grid

The effect of fluid attraction in the simulation

Two cylinders with a diameter of 0.05 meters at 0.025 meters from each other were configured to rotate in opposite directions, e.g., one cylinder was configured to rotate counterclockwise and the other one – clockwise. The flows converged between the cylinders, maintaining a circulation velocity greater than zero, and lowering the pressure between them (Fig. 11). The circulation rate of the fluid flow between the cylinders did not decrease to zero, it was maintained by the circulation of the adjacent cylinder (Fig. 12). The pressure difference $P_{outer}=P_1$ outside the cylinders and $P_{inner}=P_2$ between the cylinders created an attractive force acting on each cylinder separately, directed from the outside of each cylinder into the interior of the space between the cylinders (Fig. 13).

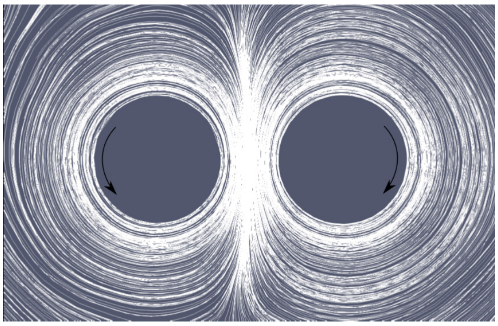

Figure 11. Tracing of airflow circulation in simulation with multidirectional rotation of the boundary layer of air

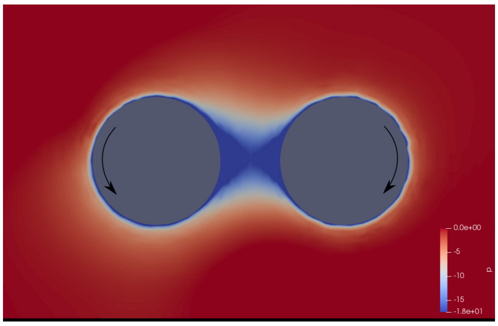

Figure 12. Distribution of airflow velocities in simulation with multidirectional rotation of the boundary layer of air

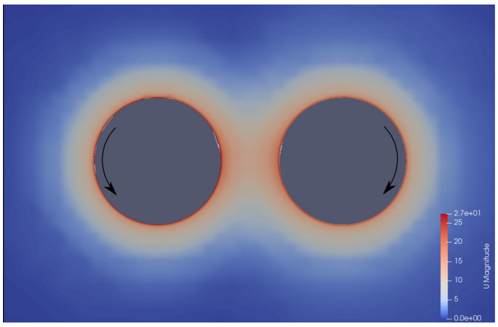

Figure 13. Distribution of air pressure in simulation with multidirectional rotation of the boundary layer of air

The force arising from the difference between external P_1 and internal pressure P_2 was calculated using the formula from the definition of pressure (6), and the pressure difference as (7) [12]:

$$P = \frac{F}{A} \quad (6)$$

$$\text{where } P = P_1 - P_2 = \triangle P_{12} \quad (7)$$

Then the force *F* is equal to the product of the pressure difference by the area of the surface experiencing pressure (8):

$$F = \triangle P_{12} A \quad (8)$$

The simulation results (Fig. 14b) demonstrate that the minimum pressure between the cylinders is (9):

$$\frac{P_2}{\rho} = -17 \; {m^2}/{s^2} \rightarrow P_2 = -17 \, {m^2}/{s^2} \times 1.185 \; kg/m^3 = -\, 20.145 \; Pa \quad (9)$$

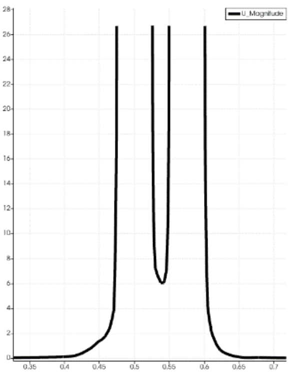

Figure 14a. Graph of airflow parameters near and between cylinders with multidirectional rotation of the boundary layer of air: Flow velocity

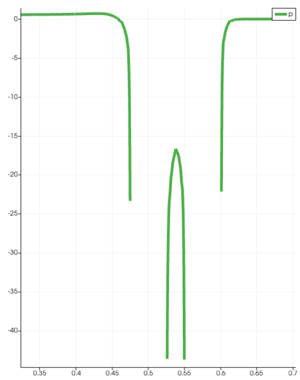

Figure 14b. Graph of airflow parameters near and between cylinders with multidirectional rotation of the boundary layer of air: Kinematic pressure

If one sets the pressure outside the cylinders to atmospheric stationary as P_1=0 Pa because numerical simulation sets the stationary pressure as 0 m^2/s^2, where the velocity of the fluids is minuscule compared to the velocity of the cylinder itself, then the pressure difference (7) relative to atmospheric is (10):

$$\triangle P_{12} = 0 - (-20.145) = 20.145 \; Pa \quad (10)$$

The contact area A of the external pressure towards the space between the cylinders is equal to half of the surface of the cylinder (11-12):

$$A = \frac{2\pi R_{cyl}}{2} * L_{cyl} \quad (11)$$

$$A = \frac{2 \times 3.1415 \times 0.025}{2} \times 0.1 = 0.00785375 \; m^2 \quad (12)$$

Using the pressure difference $\triangle P_{12}$ (10) and the contact area *A* (12), the force $F_{air\_attract}$ is calculated as (13):

$$F_{air\_attract} = 20.145 \times 0.00785375 = 0.158 \; H \quad (13)$$

Using the values (12; 18), the force F_{water} is calculated. For this, the authors of this study set P_1=0 Pa for water as well as for air, and the main characteristics of water at 25 as (14; 15; 16):

$$\rho_{water} = 997.3 \; kg/m^3 \quad (14)$$

$$\mu_{water} = 0.903 \times 10^{-6} \; m^2/s \quad (15)$$

$$\eta_{water} = \rho_{water} \times \mu_{water} = 0.901 \times 10^{-3} \; kg/(m \times s) \quad (16)$$

The kinematic pressure between the cylinders was given from the graph (Fig. 15) and was reduced to a change in dynamic pressure (17; 18; 19).

$$\frac{P_2}{\rho} = -9.5 \; {m^2}/{s^2} \quad (17)$$

$$P_2 = -9.5 \, {m^2}/{s^2} \times 997.3 \; {kg}/{m^3} = -9{,}474.4 \; Pa \quad (18)$$

$$\triangle P_{12} = 0 - (-9{,}474.4) = 9{,}474.4 \; Pa \quad (19)$$

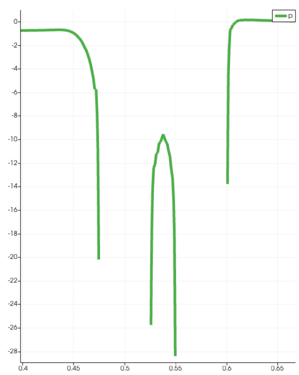

Figure 15. A graph of the kinematic pressure of the water flow near and between the cylinders in a simulation with a multidirectional rotation of the boundary layer of air

Using the dynamic pressure difference $\triangle P_{12}$ and the contact A area, the force $F_{water\_attract}$ is calculated as (20):

$$F_{water\_attract} = 9{,}474.4 \times 0.00785375 = 74.4\ H \quad (20)$$

A graph is given for a visual analysis of the difference in the rate of change of kinematic pressure for water and air in the interval between the cylinders with multidirectional rotation, from 0 to 3 seconds (Fig. 16).

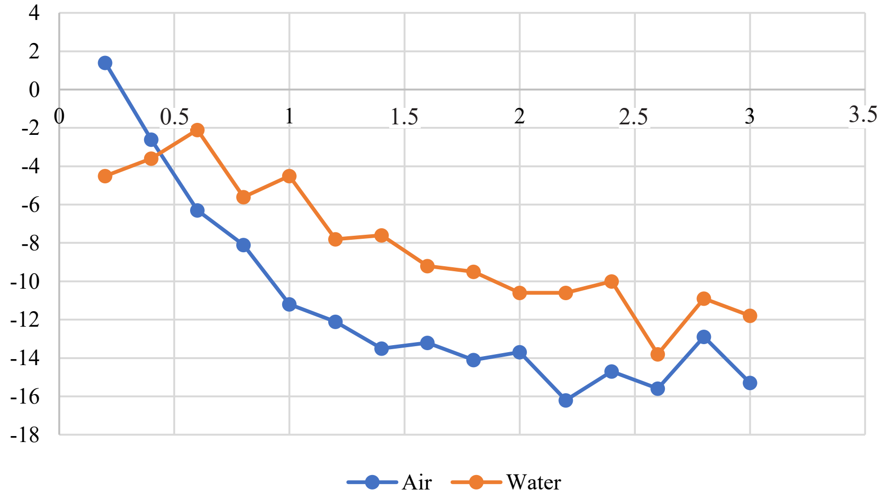

Figure 16. A graph of the pressure drop between the cylinders over time in a simulation with a multidirectional rotation of the boundary layer of air and water

The effect of fluid repulsion in the simulation

Both cylinders are configured to rotate in the same directions, e.g., one cylinder was configured to rotate counterclockwise, and the other one – clockwise. As the velocity increased, their boundary layers accelerated the airflow around each of them, forming separate airflows in the form of concentric circles. Bringing the cylinders closer as the velocity of the boundary layer increases, the airflows around the cylinders combine to form a single flow (Fig. 17). But not all the flow moved in a laminar fashion around the cylinders. The airflows at the boundary layer of the cylinder, pressed down by the external atmospheric pressure, were still trying to move around each of the cylinders. But trying to move between the cylinders, they met an oncoming flow from the neighbouring cylinder. This collision of flows stopped circulation in the centre and created excess pressure between the cylinders (Fig. 18). This excess pressure was greater than atmospheric pressure, and it enabled both cylinders to tend to push off from the zone between the cylinders. In addition, due to the collision of oncoming circulation flows, the flow velocity between the cylinder tended to zero (Fig. 19).

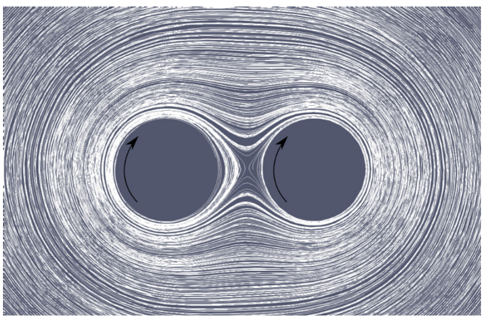

Figure 17. Tracing of airflow circulation in simulation with unidirectional rotation of the boundary layer of air

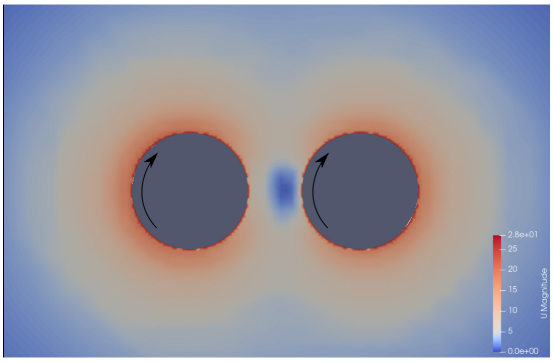

Figure 18. Distribution of airflow velocities in simulation with unidirectional rotation of the boundary layer of air

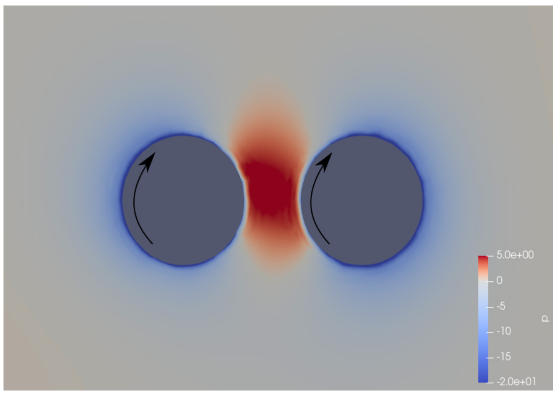

Figure 19. Distribution of air pressure in the simulation with unidirectional rotation of the boundary layer of air

Using formulas (7; 8; 11) and data from the graph (Fig. 20a, 20b), the dynamic pressure difference $\triangle P_{12air}$ $\triangle P_{12water}$ was calculated as (21; 22; 24; 25), and the repulsive forces were F_{air_repel} F_{water_repel} calculated as (23; 26):

$$\frac{P_{2\_air}}{\rho} = -5.5\ {m^2}/{s^2} \rightarrow P_{2\_air} = -5.5\ {m^2}/{s^2} \times 1.185\ kg/m^3 = -\ 6.5\ Pa \quad (21)$$

$$\triangle P_{12\_air} = 0 - (-6.5) = 6.5\ Pa \quad (22)$$

$$F_{air\_repel} = 6.5 \times 0.00785375 = 0.051\ H \quad (23)$$

$$\frac{P_{2\_water}}{\rho} = -6.5\ {m^2}/{s^2} \rightarrow P_{2_{water}} = -6.5\ {m^2}/{s^2} \times 997.3\ kg/m^3 = -\ 6{,}482.5\ Pa \quad (24)$$

$$\triangle P_{12_{water}} = 0 - (-6{,}482.5) = 6{,}482.5\ Pa \quad (25)$$

$$F_{water\_repel} = 6{,}482.5 \times 0.00785375 = 51\ H \quad (26)$$

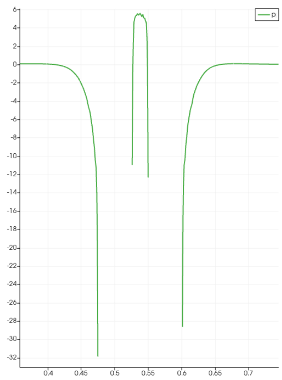

Figure 20a. A graph of the kinematic pressure of the flow near and between the cylinders in a simulation with unidirectional rotation of the boundary layer for air

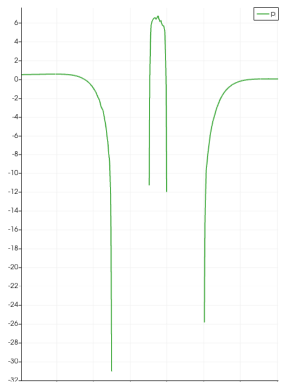

Figure 20b. A graph of the kinematic pressure of the flow near and between the cylinders in a simulation with unidirectional rotation of the boundary layer for water

Conclusions

The results obtained using numerical methods confirmed the presence of a pressure difference that causes the effects of attraction and repulsion in a fluid medium of two or more rotating cylinders. This study has proven that the effects are more pronounced in water compared to air. There is also a direct dependence of the force of interaction on the density of the medium, on the speed of rotation of the cylinders and the distance between the cylinders, which directly affect the difference between the pressure generated outside and inside between the cylinders. Kinetic viscosity affects the speed of pressure change. The lower the kinetic viscosity, the slower the molecules of the medium transmit momentum further away from the cylinders, and it will take longer to achieve the greatest pressure difference. Air has a higher kinematic viscosity, so it reaches its greatest pressure difference faster, and water is slower. But in water, due to the high density, a large force of interaction is achieved. Upon solving technical problems of contactless and non-magnetic interaction, an aqueous medium or an environment with a higher density is more suitable, which causes a greater force of effects.

The author of this paper sees the continuation of research in creating a model of magnet configurations, e.g., the Halbach array, in simulation, as well as a physical experiment with micromotors and cylinders to analyse the difference in the behaviour of magnetic field lines in the Halbach array and the cylinder assembly in the air.

References

[1] Hussain KTI, Jothi TJS. Vortex ring propagation and interactions studies. *S dhan .* 2018;(43):9. doi: 10.1007/s12046-018-0843-9.

[2] Watson EJ. The rotation of two circular cylinders in a viscous fluid. *Mathematika*. 1995;(42):105-26.

[3] Tanasheva TN, Nussupbekov BR, Dyusembaeva AN, Shuyushbayeva NN. (2019). Analysis of aerodynamic characteristics of two parallel rotating cylinders. *Technical Physics*. 2019;(64):947-9. doi: 10.1134/S1063784219070247.

[4] Hills CP. Flow patterns in a two-roll mill. *The Quarterly Journal of Mechanics and Applied Mathematics*. 2002;55(2):273-96. doi: 10.1093/qjmam/55.2.273.

[5] Price TJ, Mullin T, Kobine JJ. Numerical and experimental characterization of a family of two-roll-mill flows. *Proc Roy Soc.* 2002;459:117-35. doi: 10.1098/rspa.2002.1022.

[6] Ren H, Zhang GX, Guan HS. Three-dimensional numerical simulation of a vortex ring impinging on a circular cylinder. *Fluid Dyn. Res.* 2015;(47):025507. doi: 10.1088/0169-5983/47/2/025507.

[7] Dritschel DG. A general theory for two-dimensional vortex interactions. *J. Fluid Mech.* 1995;(293):269-303.

[8] Speight J. Rules of thumb for petroleum engineers. Kinematic Viscosity. Beverly: Scrivener Publishing; 2017. 755 p. doi: 10.1002/9781119403647.ch209.
[9] Childs PRN. Rotating Flow. Philadelphia: Elsevier Inc; 2011. 389 p.
[10] Melnykova ON. Channel flow dynamics. Moscow: Max Press; 2006. 133 p.
[11] Leweke T, Le Dizes S, Williamson CHK. Dynamics and instabilities of vortex pairs. *Annual Review of Fluid Mechanics*. 2016;(48):507-41. doi: 10.1146/annurev-fluid-122414-034558.
[12] Le Dizès S, Verga, A. Viscous interactions of two co-rotating vortices before merging. *Journal of Fluid Mechanics*. 2002;(467):389-410. doi: 10.1017/S0022112002001532.
[13] Johnson HG, Brion V, Jacquin L. Crow instability: Nonlinear response to the linear optimal perturbation. *Journal of Fluid Mechanics*. 2016;(795):652-70.
[14] Dormy E, Moffatt HK. Flow induced by the rotation of two circular cylinders in a viscous fluid. *Fluid Dynamics;* 2020. doi: 10.48550/arXiv.2008.04432.
[15] Gadzhiev DA, Gaifullin AM, Zubtsov AV. On vortex generation by a rotating cylinder. *Fluid Dynamics*. 2020;(55):965-81. doi: 10.1134/S0015462820080042.
[16] Armengol J, Calbó J, Pujol T, Roura P. Bernoulli correction to viscous losses. Radial flow between two parallel discs. *American Journal of Physics*. 2008;76(8):730.

Ефекти відштовхування і притягнення між обертовими циліндрами у флюїдах

Вадим Олексійович Останін

Анотація

Актуальність. З теорії гідродинаміки відомо про взаємодію пари вихорів у нев›язких флюїдах. Актуальність дослідження обумовлена наявністю досліджень численних симуляцій взаємодій двох вихорів або двох циліндрів, які не досліджують практичні установки для спостереження ефектів притягнення та відштовхування у флюїдних середовищах, що може гальмуати дослідження в цій області для практичного застосування.

Мета. Метою цього дослідження є практична демонстрація можливості ефекту подвійної взаємодії в повітрі з вирахуванням приблизної величини сили, яка намагається притягнути або відштовхнути циліндри.

Методи. У практичному експерименті використовується пара пластикових циліндрів, які приводяться в рух двигунами і обертаються один поруч з іншим у повітрі при атмосферному тиску. Числове моделювання ефекту показує природу ефекту і дозволяє передбачити величину сили, створюваної циліндрами, що обертаються один до одного. Зв'язок між напрямками обертання циліндрів і спостережуваними ефектами було перевірено численним розрахунком за допомогою численного моделювання конечних об›ємів у OpenFOAM версії 9.

Результати. У практичному експерименті пара циліндрів, що обертаються починала взаємодію на відстані 5–7 см, та за відстані 2–3 см створювало достатню силу, аби стабілізувати коливання одного з циліндрів навколо нитки, за яку він підвішений. Численна симуляція показує, що в просторі циліндрами утворюється зона високого або низького тиску в залежності від напрямку обертання. Обертання сусідніх дисків з протилежними напрямками руху допомагає циркуляції іншого циліндра підтримувати швидкість потоку в зазорі, що знижує тиск рідини між циліндрами і притягує їх. І навпаки, циліндри, що обертаються в одному напрямку гасять і стискають рідинні потоки в шпарині, що збільшує тиск повітря між циліндрами, що обертаються, вище стаціонарного тиску і відштовхує їх.

Висновки. Результати дають можливість детальніше розуміти процеси флюїдної взаємодії, досліджувати залежність сили від впливу середовища та циліндрів і показують параметри практичної можливості застосування ефектів взаємодії в рідинних середовищах

Ключові слова: взаємодія циркуляції, флюїдні вихори, обертання циліндрів, численна симуляція